


Article

Thermodynamics of Imidazolium-Based Ionic Liquids for Inhibiting the Spontaneous Combustion of Sulfide Ore

Jiaxin Tian¹, Kai Pan¹, Zhihui Lang¹, Rui Huang¹, Wenrui Sun¹, Hanyu Chu¹, Haotong Ren¹, Lingyu Dong¹, Yawen Li¹, Haining Wang¹ and Hui Liu^{1,2,*} 

¹ College of Quality and Safety Engineering, China Jiliang University, Hangzhou 310018, China; t.jx729@gmail.com (J.T.); pankai9826@gmail.com (K.P.); lzh18621@gmail.com (Z.L.); huangrui8782@gmail.com (R.H.); swrui.sun@gmail.com (W.S.); chy0830vivian@gmail.com (H.C.); rht423@gmail.com (H.R.); misayalingk@gmail.com (L.D.); yawen944@gmail.com (Y.L.); whnfyy@cjl.u.edu.cn (H.W.)

² State Key Laboratory Cultivation Base for Gas Geology and Gas Control, Henan Polytechnic University, Jiaozuo 454000, China

* Correspondence: hui.liu@cjl.u.edu.cn

Abstract: Spontaneous combustion of sulfide ore is one of the most common disasters in the process of ore mining, storage, and transportation, which can lead to a series of safety and environmental problems, thus affecting sustainable development in society. In this paper, four imidazolium-based ionic liquids: [BMIM][I], [BMIM][BF₄], [EMIM][BF₄], and [BMIM][NO₃], were selected for inhibition experiments with sulfide ores to reveal the inhibition performance of ionic liquids against spontaneous combustion. The results show that the main products from the reaction were Fe₂O₃ and SO₂, produced during the process of oxidation and spontaneous combustion and that the reaction moves towards a higher temperature under the action of ionic liquid, indicating that ionic liquids have a significant inhibition effect on the spontaneous combustion of sulfide ore. At the same temperature, the apparent activation energies of the samples treated with ionic liquids were all greater than those of the control samples, indicating that imidazolium-based ionic liquids can effectively reduce the spontaneous combustion tendency of sulfide ores. In addition, compared with other ionic liquids, [BMIM][NO₃] had a more pronounced inhibition effect, with the activation energies of both ore samples maximally increased by 8.4% and 10.2% after [BMIM][NO₃] treatment. This is due to the ability of [BMIM][NO₃] to better isolate the samples from oxygen in the air and reduce the effective collisions between active molecules, thus inhibiting and retarding the spontaneous combustion of sulfide ores.

Keywords: sulfide ores; spontaneous combustion; thermodynamics; ionic liquids; inhibition



check for updates

Citation: Tian, J.; Pan, K.; Lang, Z.; Huang, R.; Sun, W.; Chu, H.; Ren, H.; Dong, L.; Li, Y.; Wang, H.; et al. Thermodynamics of Imidazolium-Based Ionic Liquids for Inhibiting the Spontaneous Combustion of Sulfide Ore. *Sustainability* **2022**, *14*, 7915. <https://doi.org/10.3390/su14137915>

Academic Editors: Chaolin Zhang, Bobo Li and Shoujian Peng

Received: 31 May 2022

Accepted: 27 June 2022

Published: 29 June 2022

Publisher's Note: MDPI stays neutral with regard to jurisdictional claims in published maps and institutional affiliations.



Copyright: © 2022 by the authors. Licensee MDPI, Basel, Switzerland. This article is an open access article distributed under the terms and conditions of the Creative Commons Attribution (CC BY) license (<https://creativecommons.org/licenses/by/4.0/>).

1. Introduction

Sulfide ores, which are important strategic industrial resources, usually refer to metal minerals containing sulfur. Common sulfide ores are pyrite, albite, magnetic pyrite, etc., among which pyrite is the most widely distributed mineral in China [1]. During the mining and storage of sulfide ore, it is easy for it to be oxidized by moist air, thus releasing a large amount of heat [2–4]. At the same time, affected by the mining stratum environment, the mining products are often accompanied by carbon powder, oil scale, and other impurities, which often form a mixture with a porous and loose structure with sulfide ore, and the heat in the mixture is more difficult to dissipate. When the ore accumulates in large quantities, and the heat dissipation conditions are poor, heat will accumulate inside the ore pile until it reaches the ignition point and causes a series of spontaneous combustion disasters [5–7]. As early as 1945, there was a spontaneous mineral sulfide fire in the Braden mine in Chile, resulting in 355 deaths [8]; In previous reports, 20–30% of pyrite and 5–10% of non-ferrous metal or polymetallic sulfide ores in China are at risk of spontaneous combustion [9,10]. For example, there have been sulfide mine fire accidents in the Wushan Mine in Jiangxi Province

and the Xiangshan Mine in Anhui Province [11]. Sulfide ore spontaneous combustion will not only cause a series of major accidents, such as cave collapse and the ignition of other minerals leading to chain explosions, endangering the lives of operators, but also leads to the loss of mineral resources and may even force some mines to close or change their mining methods and processes, causing large-scale economic losses [5], and thus affect the sustainable development of society. Therefore, the problem of the spontaneous combustion of sulfide ore has become one of the more important works of disaster prevention and control in the process of sulfide ore mining and storage and transportation.

At present, the research on sulfide ore spontaneous combustion disaster prevention and control mainly includes the study of the spontaneous combustion mechanism of sulfide ore [12,13], the study of sulfide ore flame suppression and damping technology [14], and the study of the technology surrounding ore spontaneous combustion prediction, fire source detection, etc. [7,11]. Among these, flame inhibition and retardant technology of the ore can essentially prevent the occurrence of spontaneous combustion disaster or weaken its severity and improve the intrinsic safety level in mining and ore storage and transportation [15]. As a new type of organic solvent, ionic liquids have the characteristics of non-volatility, high specific heat capacity, and high thermal stability, which all have significant effects on flame suppression and chemical resistance [16–19]. Deng et al. [16] investigated the combustion mass loss and heat release rate of coal samples treated with two ionic liquids: [BMIM][BF₄], and [BMIM][I] and proposed the optimal mass ratio of ionic liquids based on economic benefits. Xi et al. [17] studied the inhibition effect of [BMIM][NTF₂] and [BMIM][BF₄] ionic liquids on the spontaneous combustion of coal. They found that the specific surface area and pore volume of coal samples treated with ionic liquids were lower, the chemical structure was more stable, and the reaction of chemical functional groups on coal surface with oxygen was more difficult. As an exception to the application of spontaneous combustion deterrence in coal, ionic liquids have been widely used as corrosion inhibitors in the field of corrosion prevention. Zheng et al. [20] studied the corrosion inhibition behavior of two ionic liquids: [OMIM]Br and [AOIM]Br, on mild steel in a sulfuric acid solution, and the results showed that both have good corrosion inhibition properties. Ionic liquids are used as corrosion inhibitors because of their ability to adsorb onto the metal surface and weaken the intensity of oxygen oxidation of the metal, whereas metal sulfide minerals tend to be metallic. Thus, we assume that it is highly feasible to inhibit the spontaneous combustion of metal sulfide minerals with the help of ionic liquids. To this end, four imidazole-based ionic liquids: [BMIM][I], [BMIM][BF₄], [EMIM][BF₄], and [BMIM][NO₃], were selected to study their inhibition performance against the spontaneous combustion of sulfide ores. Microstructure changes of sulfide ore samples after ionic liquid treatment, thermal analysis experiments, and a reaction kinetic model were used to comprehensively analyze the inhibition performance and mechanism of ionic liquids on the spontaneous combustion of sulfide ores. The research results are of great practical significance to the prevention and control of spontaneous combustion hazards in the process of sulfide-ore mining, storage, and transportation.

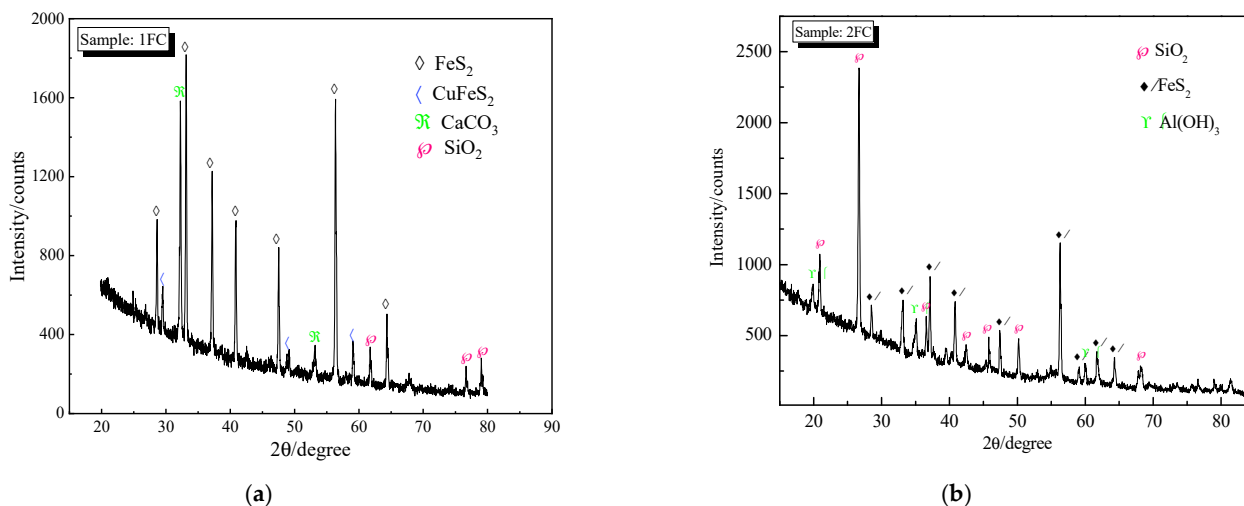
2. Experiments and Methods

2.1. Sample Preparation

In this experiment, two representative samples were collected from a mining area in Jiangxi, China. To prevent the oxidation of the ore samples caused by the high temperature generated by mechanical grinding, we used manual crushing to obtain the experimental samples, which were marked as 1FC and 2FC, respectively. The elemental analysis results of the ore sample are shown in Table 1. It can be seen that Fe and S elements account for the highest proportion in the ore sample, and there are also a few other elements present, such as C, F, N, O, Cu, Ca, and Al. Combined with the XRD diagram of the ore samples in Figure 1, we can infer that the main component of the two ore samples is FeS₂, and the impurities present are mainly SiO₂, Al(OH)₃, and oxides of various metals.

Table 1. Elemental analysis of ore samples (mass fraction/%).

Sample	C	S	Fe	F	N	O	Cu	Ca	Al
1FC	4.55	45.12	43.47	1.38	0.89	2.71	1.05	0.20	0.63
2FC	4.47	42.14	42.04	1.39	1.84	5.75	0.87	0.11	1.39

**Figure 1.** XRD patterns of the two ore samples, (a) 1FC and (b) 2FC.

2.2. Experimental Equipment and Methods

In this paper, four ionic liquids were selected for the research on spontaneous combustion inhibition of sulfide ores and their physicochemical properties are shown in Table 2. The methods of treating ore samples with ionic liquids are as follows: First, 10 g of the two ore samples pretreated in Section 2.1 were taken and placed in two beakers, mixed with IL1 at a 1:2 mass ratio, and placed on a magnetic stirrer, setting the stirrer speed to 500 r/min, stirred for 8 h in the dark and stored in a refrigerator at 5 °C under the condition of avoiding light. We then repeated the above operations to treat two ore samples, respectively, with ILs 2, 3, and 4. After leaving the treated sample for 2 days, the sample was pumped and filtered, and the filtered sample was dried via a dryer for 3 h. The dried samples were bagged separately and stored in a sealed, dry, and dark environment.

Table 2. Four kinds of ionic liquids used in the inhibition of spontaneous combustion of sulfide ores.

Number of Ionic Liquids	Chemical Expression	Melting Point of Ionic Liquids	Storage Condition	CAS Number
IL1	$C_8H_{15}IN_2$	−72 °C	Protection from light, inert gas, room temperature	65039-05-6
IL2	$C_8H_{15}BF_4N_2$	−71 °C	Below 30 °C	174501-65-6
IL3	$C_6H_{11}BF_4N_2$	15 °C	Sealed dry, room temperature	143314-16-3
IL4	$C_8H_{15}N_3O_3$	18 °C	Ventilation, low temperature, drying	179075-88-8

Thermal analysis techniques have been widely used to characterize the spontaneous combustion characteristics of ferric sulfide compounds, among which thermogravimetric (TG) is usually used to study the kinetic parameters of ferric sulfide compounds burning at high temperatures [21]. A STA-8000 synchronous thermal analyzer was used to conduct thermogravimetric experiments on the samples treated with ionic liquid and the samples in the control group in this experiment. The samples of 50 mg were placed in an alumina

crucible, setting the heating rate to 15 °C/min and 20 °C/min, and heated up from room temperature to 700 °C. The scanning gas was air, the protective gas was nitrogen, and the gas flow rate was controlled at 20 mL/min.

2.3. Thermodynamic Theory

Thermal analysis kinetics is a method of obtaining thermodynamic parameters and reaction mechanism functions through thermal analysis techniques [12]. Among them, solid-phase reaction kinetics constitutes the core of thermal analysis kinetics research, with the main task of determining the mechanism of the reaction and related kinetic parameters. According to the kinetic theory of thermal analysis, the spontaneous combustion reaction of sulfide ore can be explained by the Arrhenius equation:

$$\frac{d\alpha}{dt} = A \exp\left(-\frac{E}{RT}\right) f(\alpha) \quad (1)$$

In the equation, α is a conversion for the quality of the test sample in $\alpha = (m_0 - m_t)/(m_0 - m_\infty)$; m_0 is the mass at the beginning of the reaction; m_t is the quality of the t moment; m_∞ is the mass at the end of the reaction; t is the time in s; T is the temperature in °C; A is the pre-exponential factor in s^{-1} ; E is the apparent activation energy in kJ/mol; R is the molar gas constant with a numerical value of $8.134 \text{ J}\cdot\text{mol}^{-1}\cdot\text{K}^{-1}$; and $f(\alpha)$ is reaction mechanism function.

Under constant heating rate conditions, the heating rate $\beta = dT/dt$ is substituted to the above equation, and Equation (2) is obtained:

$$\frac{d\alpha}{f(\alpha)} = \frac{A}{\beta} \exp\left(-\frac{E}{RT}\right) dT \quad (2)$$

2.3.1. The Most Probable Mechanism Function Inference

In thermal analysis kinetics, the use of the Malek method reduces the workload of the calculation on a case-by-case basis when determining the mechanism function of the ore sample in the oxidative spontaneous combustion stage. Moreover, at the same time, this method avoids the trouble of the kinetic compensation effect when the activation energy (E_a), pre-exponential factor (A), and the mechanism function ($f(\alpha)$) are obtained simultaneously [12,22]:

$$y(\alpha) = \left(\frac{T}{T_{0.5}}\right)^2 \times \frac{\frac{d\alpha}{dt}}{\left(\frac{d\alpha}{dt}\right)_{0.5}} = \frac{f(\alpha) \times G(\alpha)}{f(0.5) \times G(0.5)} \quad (3)$$

$$f(\alpha) = \frac{1}{dG(\alpha)/d\alpha} \quad (4)$$

In the equation, $y(\alpha)$ is the defined function; α is conversion rate; T is the temperature corresponding to α in °C; $T_{0.5}$ is the temperature at $\alpha = 0.5$; $f(\alpha)$ and $G(\alpha)$ are the differential and integral forms of the mechanism functions, respectively; $d\alpha/dt$ is reaction rate, and $(d/dt)_{0.5}$ is the reaction rate at $\alpha = 0.5$. Substituting the experimental test values and each mechanism function to the left and right of Equation (3), respectively, gives the experimental and standard curves. When the deviation between the experimental and standard curves is minimum, its corresponding mechanism function is the most probable. Table 3 describes common reaction mechanism functions and kinetics model [23].

Table 3. Reaction mechanism functions for thermal analysis kinetics.

Number	Function Name	Mechanism	$f(\alpha)$	$G(\alpha)$
1	Chemical Reaction	$n = 2$	$(1 - \alpha)^2$	$(1 - \alpha)^{-1} - 1$
2	Chemical Reaction	$n = 3$	$(1 - \alpha)^3$	$[(1 - \alpha)^{-2} - 1]/2$
3	Chemical Reaction	$n = 4$	$(1 - \alpha)^4$	$[(1 - \alpha)^{-3} - 1]/3$
4	Valensi equation	Two-dimensional diffusion	$-1/\ln(1 - \alpha)$	$\alpha + (1 - \alpha)[\ln(1 - \alpha)]$
5	Ginstling-Brounshtein equation	Three-dimensional diffusion	$3/2[(1 - \alpha)^{1/3} - 1]^{-1}$	$1 - 2\alpha/3 - (1 - \alpha)^{2/3}$
6	Shrinkage geometrical column	Two-Dimensional Phase Interfacial Reaction	$2(1 - \alpha)^{1/2}$	$1 - (1 - \alpha)^{1/2}$
7	Shrinkage geometrical spherical	Three-Dimensional Phase Interfacial Reaction	$3(1 - \alpha)^{2/3}$	$1 - (1 - \alpha)^{1/3}$
8	Mamplé law	Nucleation and growth	$1 - \alpha$	$-\ln(1 - \alpha)$
9	Power law	$n = 1/3$	$3\alpha^{2/3}$	$\alpha^{1/3}$
10	Power law	$n = 1/4$	$4\alpha^{3/4}$	$\alpha^{1/4}$

2.3.2. Calculation of Activation Energy and Pre-Exponential Factor

The iso-conversion method [24,25] can solve the thermal analysis kinetic parameters by comparing the thermogravimetric data corresponding to the same α value at two sets of different heating rates, and the effects of the functions of unknown mechanisms can be eliminated. In this thesis, the Friedman method [26] was used to solve for reaction kinetic parameters, and Equation (5) was obtained by taking the logarithm on both sides of Equation (2). At the same conversion rate, there is a linear relationship between $\ln(\beta d\alpha/dT)$ and $1/T$ with different heating, and its slope is $-E/R$.

$$\ln\left(\beta \frac{d\alpha}{dT}\right) = \ln[Af(\alpha)] - \frac{E}{RT} \quad (5)$$

When using differential methods to solve kinetic parameters for thermal analysis, the arch method [22] was selected for the calculations in this paper. After separating the variables for Equation (2), the Achar equation can be obtained by taking logarithms on both sides, as shown in Equation (5), where $\ln[(d/dT)/f(\alpha)]$ was linearly related to $1/T$, and the slope was $-E/R$ and the intercept was $\ln(A/\beta)$. The calculation is performed by substituting different $f(\alpha)$ into Equation (5) and fitting linearly; the apparent activation energy E and the pre-exponential factor A can be obtained.

$$\ln \frac{d\alpha}{f(\alpha)dT} = \ln \frac{A}{\beta} - \frac{E}{RT} \quad (6)$$

When using the integral method to solve for thermal analysis kinetic parameters, the Coats–Redfern equation [22] approximation (9) was used for calculations in this paper, which can be obtained by combining the logarithm Frank–Kamenetskii [22] approximations (7) and Equation (8).

$$\int_0^T \exp\left(-\frac{E}{RT}\right) dT = \frac{RT^2}{E} \exp\left(-\frac{E}{RT}\right) \quad (7)$$

Integral to Equation (2) was obtained:

$$\int_0^\alpha \frac{d\alpha}{f(\alpha)} = G(\alpha) = \frac{A}{\beta} \int_0^T \exp\left(-\frac{E}{RT}\right) dT \quad (8)$$

After substituting Equation (7) into Equation (8) and taking the logarithm:

$$\ln\left(\frac{G(\alpha)}{T^2}\right) = \ln\left(\frac{AR}{\beta E}\right) - \frac{E}{RT} \quad (9)$$

Similar to the differential methods, the slope and intercept were obtained by linear fitting of the above formula, and the apparent activation energy and pre-exponential factor of the oxidation spontaneous combustion process of ore samples were obtained.

3. Results and Discussions

3.1. Effects of Ionic Liquids on the Microstructure of Sulfide Ores

3.1.1. Effect of Ionic Liquids on the Micromorphology of Sulfide Ores

To analyze the effect of ionic liquids on the micromorphology of the ore samples, the ore samples inhibited by ionic liquids were magnified to a magnification of 2K using a Sigma 300 electron scanning microscope, as shown in Figures 2 and 3, with the control group treated with water in Figures 2 and 3a. It can be seen that in the control group (a), the surface of the ore sample particles is flat with a few fine particles present around it, and the pore structure is not apparent. Compared with the control group samples, some pores appeared on the surface of the samples after inhibition, the surface roughness increased to different degrees, and the fine particles attached around the large particles increased. In general, the surface morphologies of the samples treated with different ionic liquids are quite different; the surface is looser than the unhindered samples, and the number of fine particles on and around the large particles had also increased.

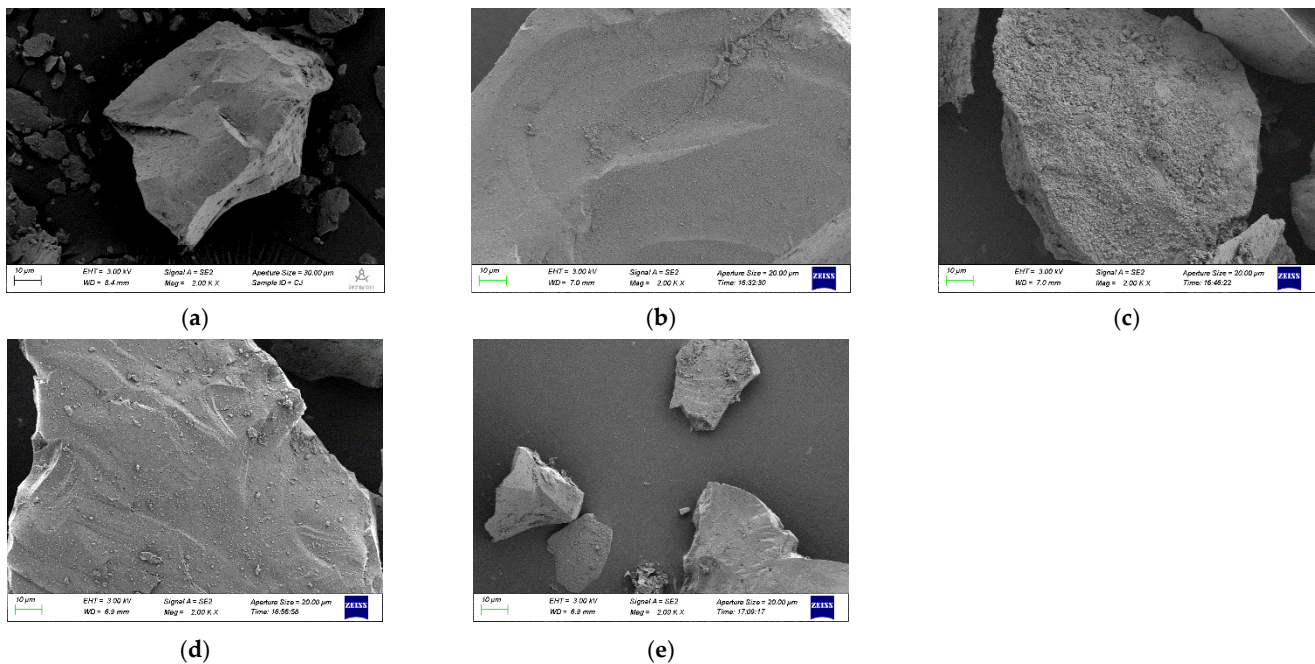


Figure 2. SEM image of the 1FC sample after treatment with water and ionic liquids. (a) Treatment with water; (b) IL1; (c) IL2; (d) IL3; (e) IL4.

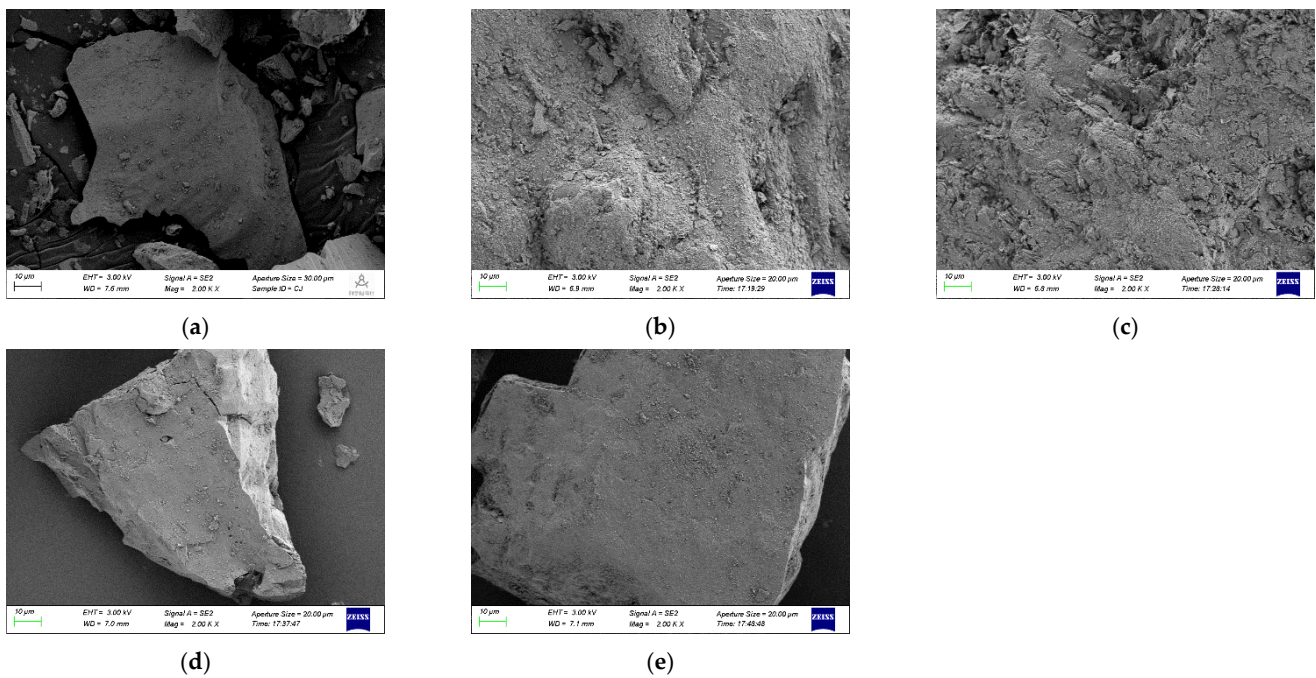


Figure 3. SEM image of the 2FC sample after treatment with water and ionic liquids. (a) Treatment with water; (b) IL1; (c) IL2; (d) IL3; (e) IL4.

3.1.2. Effect of Ionic Liquid Blocking on the Microscopic Elemental Composition of Sulfide Ores

The XRD maps of the four samples treated with ionic liquid were measured by X-ray diffractometer analysis, as shown in Figure 4. As can be seen from the XRD pattern, the diffraction peak positions of the ore samples are essentially the same, with only a few diffraction peaks showing variation, indicating that the ionic liquid does not react with the significant elements in the sulfide ore. Based on the data in the graph, it can be seen that most of the diffraction peaks of the samples have decreased in value and increased in width after ionic liquid treatment, which indicates that the ionic liquid treatment led to the change of the crystal structure of the mineral and the arrangement of atoms in the mineral crystal. Table 4 shows the results of the elemental analysis of each sample after being inhibited by the ionic liquid, and it can be seen that the percentage of Fe and S elements in the sample remains the highest after treatment with ionic liquid, with small amounts of C, N, I, and F also found in the samples, which can be inferred to be ionic liquid residues according to the ionic liquid chemical expression.

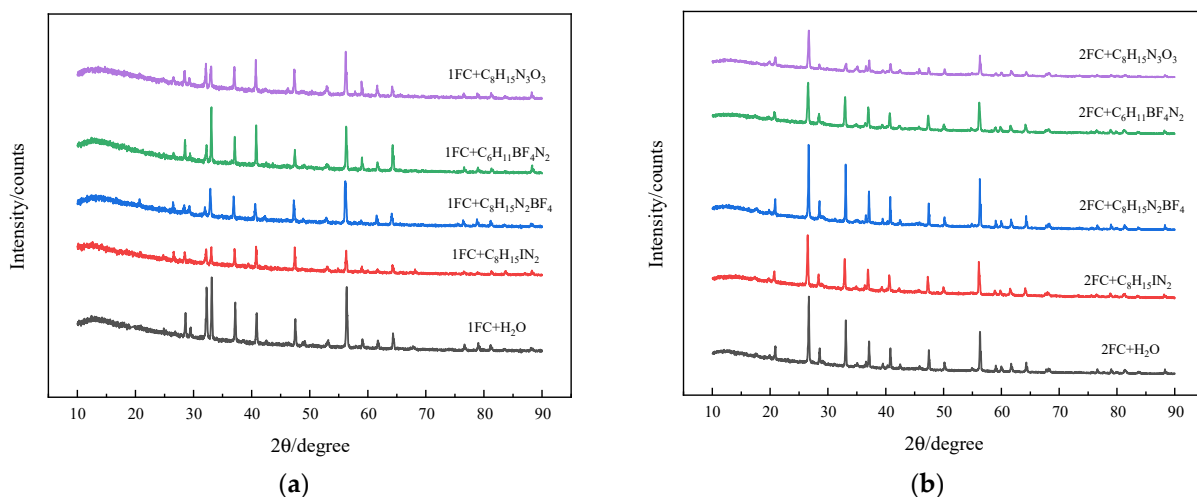


Figure 4. XRD patterns of individual ore samples after treatment with ionic liquids. (a) 1FC; (b) 2FC.

Table 4. Elemental analysis of the ore samples (mass fraction/%).

Sample	C	S	Fe	F	N	I	O	Cu	Ca	Al
1FC-IL1	5.44	40.10	48.87	0.85	1.75	0.27	0.47	0.88	0.35	1.02
1FC-IL2	8.23	45.86	40.92	2.26	1.00	0.00	0.52	0.54	0.09	0.58
1FC-IL3	8.33	43.66	39.66	2.34	0.33	0.04	3.53	0.49	0.07	1.55
1FC-IL4	6.24	46.78	42.48	1.58	0.02	0.00	1.56	0.43	0.03	0.88
2FC-IL1	2.78	45.37	42.61	2.38	2.79	0.00	1.99	0.78	0.11	1.19
2FC-IL2	5.29	44.48	41.73	2.65	1.71	0.00	2.43	0.66	0.09	0.96
2FC-IL3	4.45	45.33	44.87	1.31	0.92	0.00	1.86	0.21	0.04	1.01
2FC-IL4	4.51	46.37	39.95	2.55	2.14	0.00	2.77	0.24	0.03	1.44

Note. FC ore sample was treated with ionic liquid.

3.2. Thermogravimetric Analysis of Ore Samples before and after Ionic Liquid Inhibition

The thermal behavior of both the ore samples treated with ionic liquids and the control group was analyzed in our work by thermogravimetric experiments under air atmosphere conditions. Figure 5 shows the curve of TG (thermogravimetric) obtained from the experiment. Combined with the weight loss rate curves in Figure 5, the spontaneous combustion process of sulfide iron ore can be roughly divided into three stages: the low-temperature heating stage (before about 400 °C), the oxidative spontaneous combustion stage (about 400 °C–700 °C), and the end of the reaction stage (after about 700 °C). To study the inhibition performance of ionic liquids on the spontaneous combustion of sulfide ores, this paper focused on the thermal behavior, and a series of important parameters of the ore samples, in the stage of oxidation and spontaneous combustion, including the initial temperature of weight loss (T1), the maximum weight loss rate point (T2), and the temperature at which the weight loss peak appears for the first time (T3).

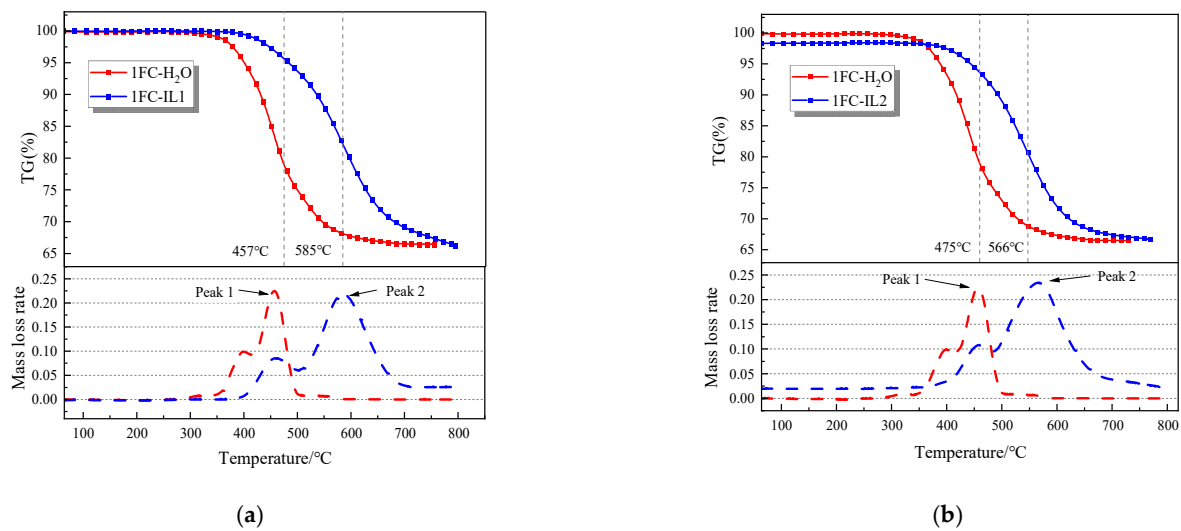
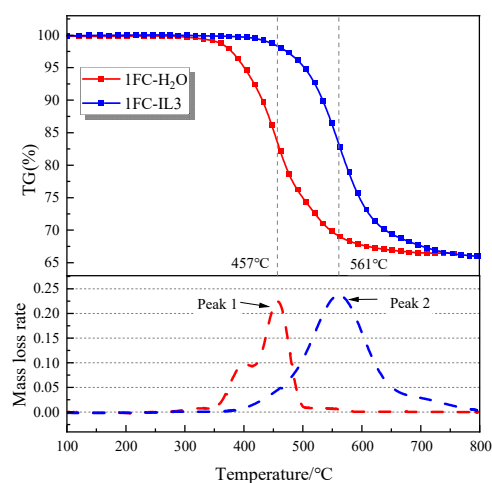
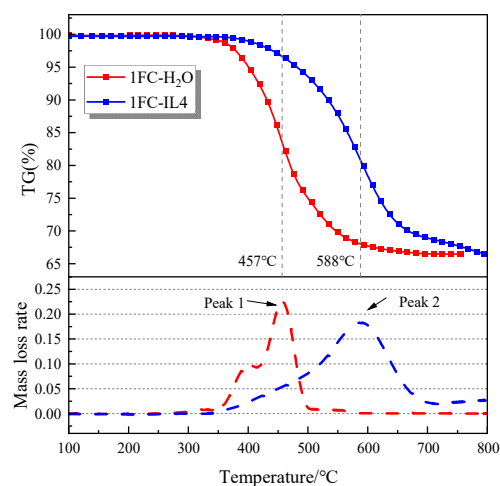


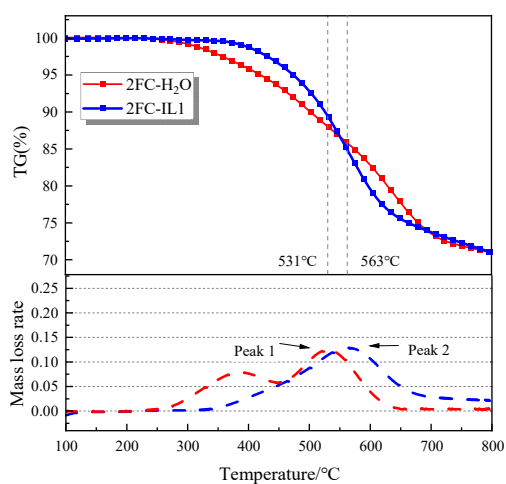
Figure 5. Cont.



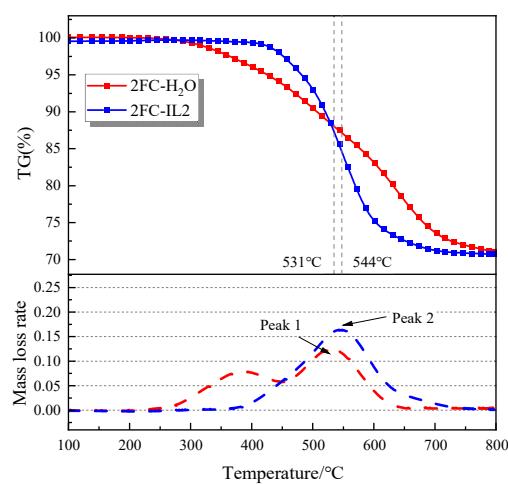
(c)



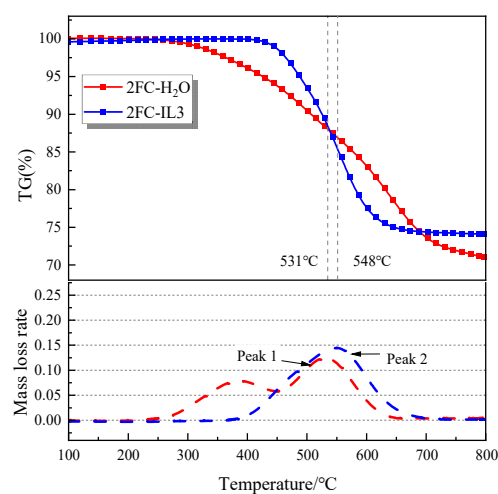
(d)



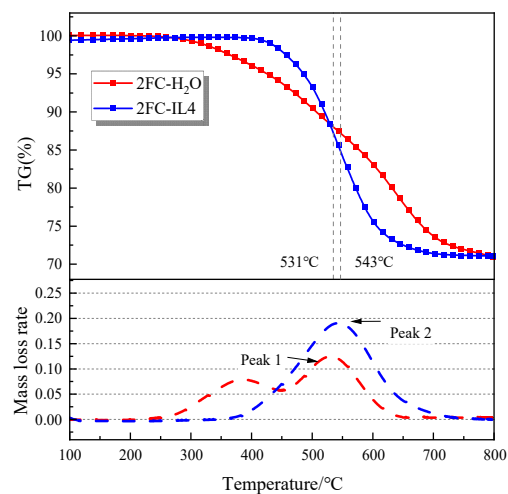
(e)



(f)



(g)



(h)

Figure 5. TG curves of ore samples treated with ionic liquids. (a) 1FC-H₂O and 1FC-IL1; (b) 1FC-H₂O and 1FC-IL2; (c) 1FC-H₂O and 1FC-IL3; (d) 1FC-H₂O and 1FC-IL4; (e) 2FC-H₂O and 2FC-IL1; (f) 2FC-H₂O and 2FC-IL2; (g) 2FC-H₂O and 2FC-IL3; (h) 2FC-H₂O and 2FC-IL4.

Two peaks can be found in the weight loss rate curves of both the control samples and some of the 1FC samples treated with ionic liquids, and the temperatures of the two peaks are relatively close. This indicates that two oxidative weight loss reactions occurred successively in these samples during the oxidative spontaneous combustion stage. These two weight loss reactions may be Equations (10) and (11), and the theoretical weight loss of Equations (10) and (11) are 33.3% and 66.7%, respectively. After combining the thermogravimetric curves with the mass fraction of FeS₂ in the sample, we found that the actual weight loss of the sample was consistent with the theoretical weight loss of the two reactions of Equations (10) and (11).



In contrast, in all of the ionic liquid treated samples from 2FC and some of the pieces from 1FC, only one weight loss peak was observed. This indicates that an oxidative weight loss reaction occurred in the oxidative spontaneous combustion stage of the samples, and the actual weight loss of all of these samples at this stage was about 30%. Combining the actual weight loss with the results of the mass fraction analysis of FeS₂ in the samples, we can infer that the oxidative weight loss reaction in Equation (11) and the oxidative weight gain reaction in Equation (12) may have occurred in these samples during the oxidative spontaneous combustion stage. The combined effect of these two reactions maintains the actual weight loss of the samples at about 30%.



The parameters of the oxidative spontaneous combustion phase were analyzed. It was found that the resistance of the four ionic liquids significantly delayed the weight loss onset temperature (T₁), as was the temperature at the point of maximum weight loss rate (T₂) and the temperature at which the weight loss peak first appeared (T₃), and that the weight loss rate curve was smoother and took longer to reach the maximum weight loss rate in the ionic liquid-treated samples than in the control samples. Therefore, based on the above changes in the thermal behavior of the ore samples after ionic liquid treatment, it can be considered that, after the treatment of ionic liquid, the overall oxidative spontaneous combustion reaction of the ore samples shifts towards higher temperatures, meaning the samples are more resistant to spontaneous combustion, indicating that ionic liquids have a better deterrent effect on the spontaneous combustion of sulfide ores. In addition, the weight loss rate of the samples treated with Ionic Liquid No. 4 was lower than that of the samples treated with other ionic liquids, suggesting that Ionic Liquid No. 4 may have the best resistance to the spontaneous combustion of sulfide ores of the four ionic liquids.

3.3. Thermodynamic Analysis of Auto-Ignition Flame Retardant

3.3.1. Solving the Most Probable Mechanism Function Based on the Malek Method

The Malek method is considered by ICTAC to reduce the scope of possible mechanism functions in the reaction without assumptions and approximations and is a superior method to infer the mechanism functions [27]. Therefore, the Malek method from Section 2.3.1 was used to analyze the reaction mechanism function of the ore samples treated with ionic liquid and the control group during the oxidative spontaneous combustion stage. After the curve obtained at a heating rate of 15 °C/min is selected, the standard curve can be obtained by substituting the differential form $f(\alpha)$ and the integral form $G(\alpha)$ of the mechanism function into the right side of the Equation (3). By substituting the thermogravimetric data of the ore samples treated with ionic liquid and the control ore samples into the left side of Equation (3), the test curve can be obtained, and the fitting results are shown in Figure 6. By comparing the correlation coefficients of ten common mechanism function standard curves and experimental test curves, we could finally infer the reaction mechanism function of

the ore samples treated by ionic liquids and the control group. That is, when the deviation between the standard curve and the experimental test curve is minimum, the corresponding mechanism function is the most probable mechanism function. In order to judge the degree of deviation between the standard and experimental curves, Origin software can be used to calculate the Pearson correlation coefficient. The larger the correlation coefficient, the smaller the degree of deviation. The calculation results are shown in Table 5.

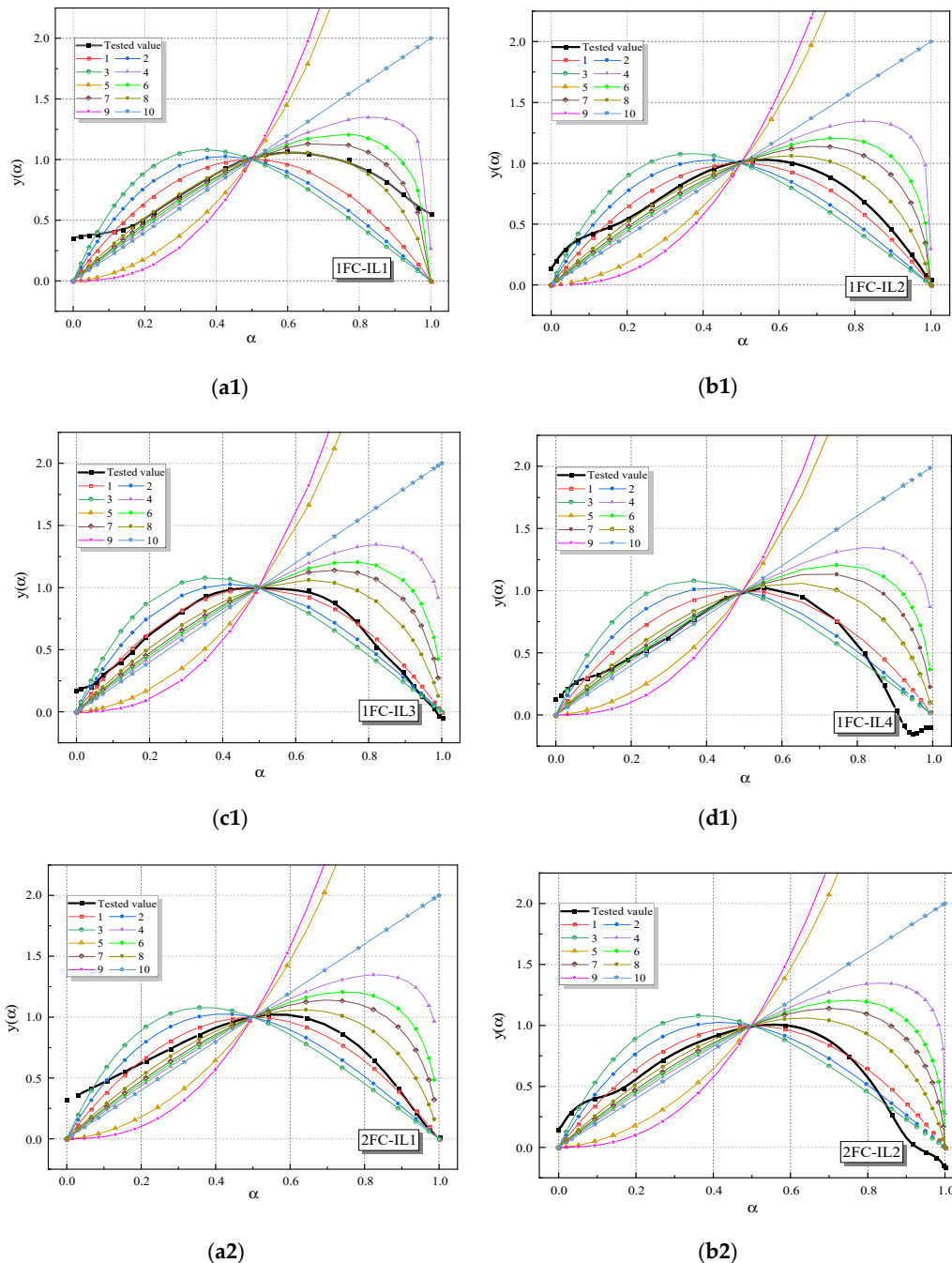


Figure 6. Cont.

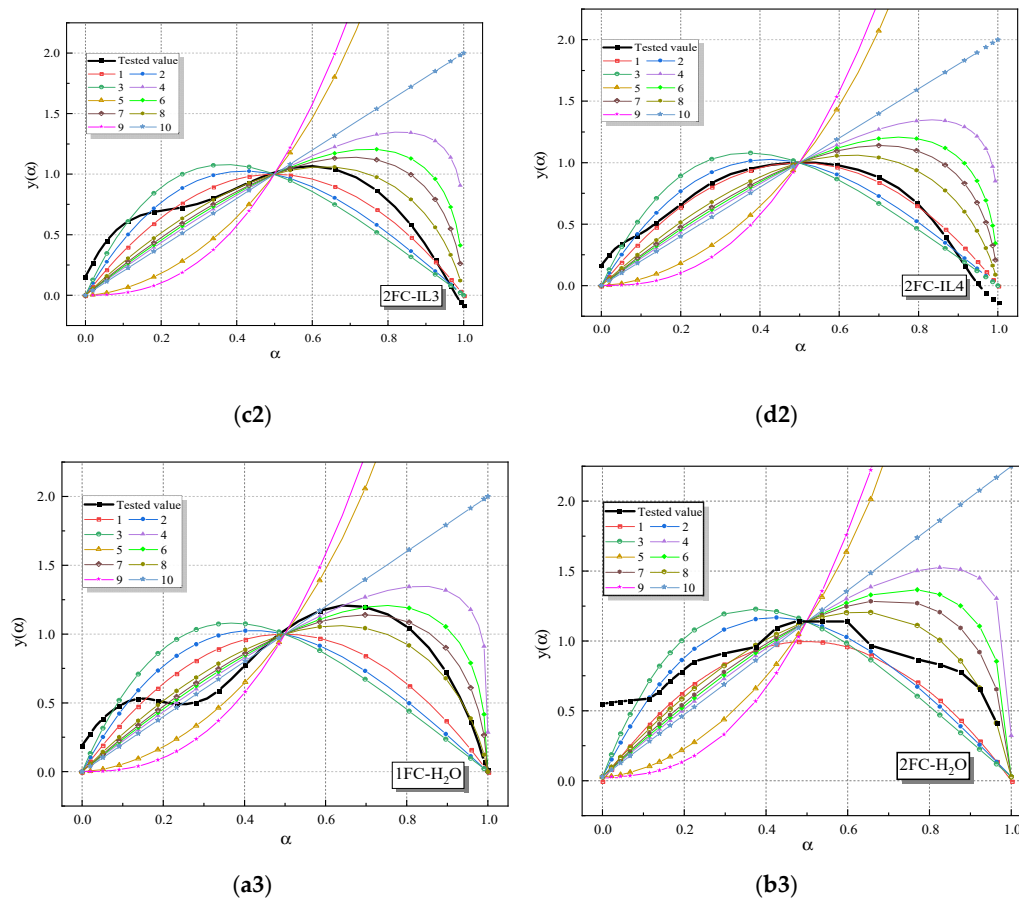


Figure 6. The fitting curve of the reaction mechanism function for the two kinds of ore samples before and after treatment. (a1) 1FC-IL1; (b1) 1FC-IL2; (c1) 1FC-IL3; (d1) 1FC-IL4; (a2) 2FC-IL1; (b2) 2FC-IL2; (c2) 2FC-IL3; (d2) 2FC-IL4; (a3) 1FC-H₂O; (b3) 2FC-H₂O.

Table 5. The correlation coefficients of the reaction mechanism function fitting for the ore samples treated.

Sample	F1	F2	F3	F4	F5	F6	F7	F8	F9	F10
1FC-IL1	0.7719	0.5978	0.4533	0.8625	0.2527	0.9220	0.9440	0.9368	0.3298	0.6094
1FC-IL2	0.9734	0.9036	0.8254	0.5349	0.2949	0.7431	0.8341	0.9380	0.2296	0.0822
1FC-IL3	0.9819	0.9603	0.9141	0.2885	0.3945	0.5581	0.6886	0.8505	0.4296	0.1476
1FC-IL4	0.9094	0.9027	0.8652	0.0417	0.6110	0.2792	0.4611	0.7039	0.5869	0.3623
1FC-H ₂ O	0.7832	0.6386	0.5287	0.6777	0.1365	0.8563	0.9041	0.9198	0.0351	0.2435
2FC-IL1	0.9573	0.9175	0.8579	0.2472	0.4816	0.5210	0.6611	0.8350	0.4999	0.2199
2FC-IL2	0.9367	0.9421	0.9143	0.0118	0.6847	0.3596	0.5270	0.7426	0.6543	0.4271
2FC-IL3	0.9492	0.9180	0.8747	0.2625	0.4658	0.5565	0.6929	0.8502	0.4810	0.1947
2FC-IL4	0.9594	0.9586	0.9289	0.0827	0.6046	0.4187	0.5834	0.7858	0.5980	0.3421
2FC-H ₂ O	0.8128	0.9070	0.9243	0.3056	0.1273	0.3933	0.4597	0.5786	0.1652	0.1787

F: Function.

According to the data in Table 5, it can be seen that the standard curve represented by mechanism function 8 (Mampelaw equation and Nucleation and growth) has the highest correlation coefficient with the experimental curve of the 1FC ore sample not treated with ionic liquid, reaching 0.9198, which is the most probable mechanism. The functional differential form is derived as $f(\alpha) = 1 - \alpha$. The correlation coefficient between the experimental curve of the 1FC ore sample treated with ionic liquid 1 and the standard curve of mechanism function 7 (shrinkage geometrical spherical equation and three-dimensional phase interfacial reaction) is the largest, and the differential form of the most probable mechanism function is $f(\alpha) = 3(1 - \alpha)^{2/3}$. The 1FC samples treated with ionic liquids 2,

3, and 4 have the highest correlation coefficient between the experimental curve and the standard curve of mechanism function 1 (chemical reaction equation, $n = 2$), and their most probable mechanism functions are all $f(\alpha) = (1 - \alpha)^2$. The correlation coefficient between the experimental curve and the standard curve of mechanism function 3 (chemical reaction equation, $n = 4$) of the 2FC ore sample not treated with ionic liquid is the largest, at 0.9243, and the most probable differential form of the mechanism function is $f(\alpha) = (1 - \alpha)^4$. The correlation coefficient between the experimental curve and the standard curve of mechanism function 1 (chemical reaction equation, $n = 2$) of the 2FC ore samples treated by ionic liquids 1, 3, and 4 is the largest, and the corresponding differential form of the mechanism function is $f(\alpha) = 1 - \alpha$. The correlation coefficient of the standard curve corresponding to the experimental curve of the 2FC ore sample treated with Ionic Liquid 2 and mechanism function 2 (chemical reaction equation, $n = 3$) is the largest, and the differential form of its most probable mechanism function is $f(\alpha) = (1 - \alpha)^3$. It is worth noting that the mechanism function of the ore samples 1FC and 2FC changed after being treated with the ionic liquid.

3.3.2. Solution of Dynamic Parameters

Based on the equal conversion rate method described above, two main reaction kinetic parameters: apparent activation energy E and pre-exponential factor A , can be calculated during the spontaneous combustion reaction of the 1FC and 2FC control ore samples. The difference between the average internal energy of active molecules and the average internal energy of all molecules is called the apparent activation energy, and the apparent activation energy is usually used as an evaluation index to distinguish the ability of a substance to spontaneously combust. In general, the smaller the apparent activation energy of a substance is, the higher its tendency to spontaneously combust [28,29]. In our work, the apparent activation energy changes in the control samples from the conversion rate of 0.1 to 0.9 were calculated at intervals of 0.1, as shown in Figure 7. It can be found that the activation energy of the control group shows a trend of rising and then decreasing with the fluctuation of the conversion rate α . In the early stage of the experiment, the oxidation activity of the ore samples is relatively high, so the apparent activation energy of the ore samples is at a lower level. With the increase in temperature, the conversion rate and apparent activation energy of ore samples gradually increased, which indicated that the reaction activity was decreasing while the active substances in the ore samples were also decreasing. When the conversion rate reached about 0.6, the apparent activation energies of the two ore samples increased rapidly. It is possible that the sample underwent a violent oxidation reaction at this point, resulting in a substantial decrease in the activity of the sample. After the conversion rate exceeded 0.6, the apparent activation energy decreases rapidly. This may be due to the increase in temperature leading to an enhancement of the reaction activity of some of the reaction products of the sample as well as other substances.

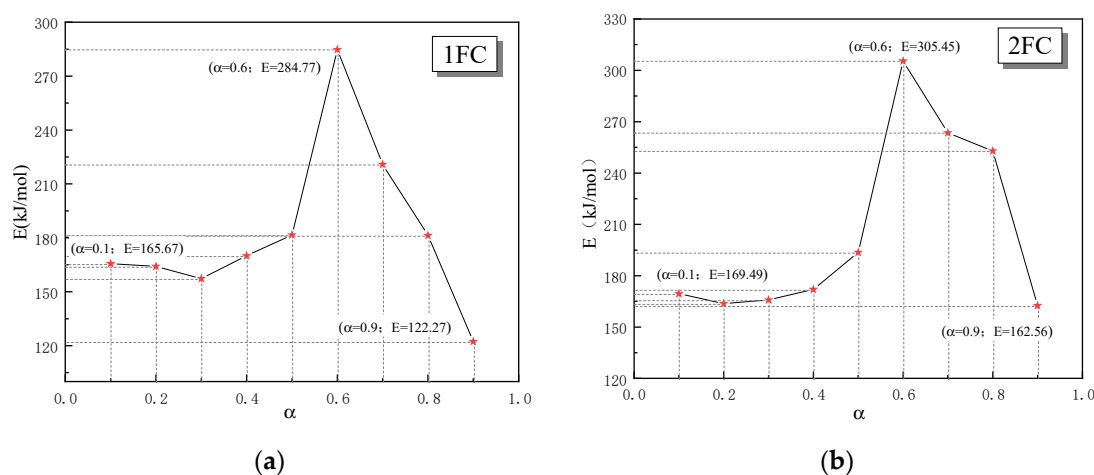


Figure 7. Apparent activation energy distribution of the control group ore samples (Note. The red asterisk indicates the activation energy at different conversion rates). (a) 1FC; (b) 2FC.

The Achar differential method and the Coast–Redfern integral method were used in our work to calculate the apparent activation energy and pre-exponential factor of the ore samples treated with ionic liquids and the control group, respectively. The results are shown in Table 6. According to Table 6, after being treated with ionic liquid, the apparent activation energy of the ore sample improved, and the spontaneous combustion tendency of sulfide ore was reduced. That is, the ionic liquid has a good inhibitory effect on the spontaneous combustion of sulfide ore. The activation energies of the 1FC samples treated with four ionic liquids: [BMIM], [BMIM][BF₄], [EMIM][BF₄], and [BMIM][NO₃], increased by 3.4%, 0.9%, 2%, and 8.4%, respectively. The activation energy of the 2FC samples increased by 4.7%, 1.3%, 3.8%, and 10.2%, respectively. Compared with the other three ionic liquids, the apparent activation energy of the two samples treated by IL4 improved the most, effectively weakening the spontaneous combustion tendency of sulfide ore and having the best inhibition effect.

Table 6. Apparent activation energy and pre-exponential factor of samples after ionic liquid treatment and control group.

Sample	E/(kJ·mol ⁻¹)	lnA
1FC-IL1	294.64	43.36
1FC-IL2	287.32	37.21
1FC-IL3	290.56	39.76
1FC-IL4	308.75	48.93
1FC-H ₂ O	284.77	32.54
2FC-IL1	319.84	52.26
2FC-IL2	309.58	41.23
2FC-IL3	317.23	32.59
2FC-IL4	336.66	43.34
2FC-H ₂ O	305.45	38.75

4. Conclusions

In this paper, the performance of ionic liquids to inhibit the spontaneous combustion of sulfide ores and the related mechanisms were investigated from both microscopic and macroscopic perspectives. A systematic study was conducted regarding four aspects: the microscopic morphology of ore samples, the oxidation spontaneous combustion process, the spontaneous combustion process mechanism, and the kinetic parameters of thermal analysis. The main conclusions are as follows:

- (1) The microstructural changes of the ore samples treated with ionic liquids and the control group were investigated by modern analytical techniques. The results showed

- that the main composition of the two samples was FeS_2 , and there were impurities such as SiO_2 and metal oxides. No new phases were generated during the treatment of the ore samples with the ionic liquids, and the elemental composition and content of the treated ore samples were not significantly different compared with the control group. However, the surface morphology of the samples differed greatly. Compared with the original samples, the surface of the samples treated with ionic liquids was looser, showing a large particle surface, and the number of fine particles had increased;
- (2) The thermal behaviors of the ore samples treated with ionic liquids and the control group were systematically analyzed by thermogravimetric techniques. The spontaneous combustion reaction process of the ore samples was similar, showing three stages: the low-temperature heating stage, the oxidized spontaneous combustion stage, and the reaction end stage. The ore samples underwent an oxidation reaction during the oxidation spontaneous combustion stage. The final reaction product was Fe_2O_3 with SO_2 gas production and intermediate products containing oxides such as FeSO_4 . After treatment with the ionic liquids, the ore samples' overall oxidative spontaneous combustion reaction moved toward a higher temperature, and the ore samples became less susceptible to spontaneous combustion. This indicates that the ionic liquid has a good inhibition effect on the spontaneous combustion of sulfide ore;
 - (3) The reaction mechanism functions and thermodynamic parameters of the ore samples treated with ionic liquids, and the control group, were obtained via the Malek, Friedman, Arch, and Coast–Redfern methods. The results show that the inhibition of the ionic liquids affected the reaction mechanism function during the oxidative spontaneous combustion stage. The activation energy of the 1FC ore samples treated with four kinds of ionic liquids increased by 3.4%, 0.9%, 2%, and 8.4%, and the activation energy of the 2FC ore samples increased by 4.7%, 1.3%, 3.8%, and 10.2%, respectively. The apparent activation energy of two ore samples increased the most after being treated with IL4, achieving the best inhibition effects.

Author Contributions: Conceptualization, H.L. and H.W.; methodology, J.T., K.P., Z.L. and H.L.; software, R.H.; validation, W.S., H.C., H.R. and L.D.; formal analysis, J.T.; investigation, J.T., K.P., H.L., Y.L. and H.W.; writing—original draft preparation, J.T.; W.S., H.C., H.R. and L.D.; writing—review and editing, K.P. and H.L.; visualization, H.W., J.T., Y.L. and K.P.; supervision, H.L. and H.W.; funding acquisition, H.L. All authors have read and agreed to the published version of the manuscript.

Funding: This work was supported in part by the Zhejiang Provincial Natural Science Foundation of China (LY22E040001), the State Key Laboratory Cultivation Base for Gas Geology and Gas Control (Henan Polytechnic University) (WS2021B06), the Fundamental Research Funds for the Provincial Universities of Zhejiang (2020YW55, 2021YW92), and the 2021 National College Students Innovation and Entrepreneurship Training Program (202110356028).

Institutional Review Board Statement: Not applicable.

Informed Consent Statement: Not applicable.

Data Availability Statement: Not applicable.

Conflicts of Interest: The authors declare no conflict of interest.

References

1. Cao, J.; Ren, S.; Wang, C.; She, J.; Jiang, Y.; Liu, Y.; Zhou, Y.; Wang, L.; Wang, J.; Wang, Y.; et al. Cadmium and lead distribution in pyrite ores: Environmental concerns over geochemically mobile fractions. *Elem. Sci. Anthrop.* **2021**, *9*, 00093. [[CrossRef](#)]
2. Li, X.; Shang, Y.; Chen, Z.; Chen, X.; Niu, Y.; Yang, M.; Zhang, Y. Study of spontaneous combustion mechanism and heat stability of sulfide minerals powder based on thermal analysis. *Powder Technol.* **2017**, *309*, 68–73. [[CrossRef](#)]
3. Liu, H.; Hong, R.; Xiang, C.; Lv, C.; Li, H. Visualization and analysis of mapping knowledge domains for spontaneous combustion studies. *Fuel* **2020**, *262*, 116598. [[CrossRef](#)]
4. Yang, F.; Lai, Y.; Song, Y. Determination of the influence of pyrite on coal spontaneous combustion by thermodynamics analysis. *Process. Saf. Environ. Protect.* **2019**, *129*, 163–167. [[CrossRef](#)]
5. Hong, R.; Liu, H.; Xiang, C.; Song, Y.M.; Lv, C. Visualization and analysis of mapping knowledge domain of oxidation studies of sulfide ores. *Environ. Sci. Pollut. Res.* **2020**, *27*, 5809–5824. [[CrossRef](#)] [[PubMed](#)]

6. Liu, H.; Wu, C.; Shi, Y. Locating method of fire source for spontaneous combustion of sulfide ores. *J. Cent. South Univ. Technol.* **2011**, *18*, 1034–1040. [[CrossRef](#)]
7. Li, Z.-J.; Shi, D.-P.; Wu, C.; Wang, X.-L. Infrared thermography for prediction of spontaneous combustion of sulfide ores. *Trans. Nonferrous Met. Soc. China* **2012**, *22*, 3095–3102. [[CrossRef](#)]
8. Stachulak, J.S. Computerized fire monitoring, criteria, techniques and experience at inco limited. *CIM Bull.* **1990**, *83*, 59–67.
9. Tang, J.H.; Feng, Y.X.; Wu, Z.L.; Zhang, S.Y.; Sarkodie, E.K.; Jin, H.M.; Yuan, R.L.; Pan, W.; Liu, H.W. Optimization studies on biological desulfurization of sulfide ore using response surface methodology. *Minerals* **2021**, *11*, 15. [[CrossRef](#)]
10. Pan, W.; Wu, C.; Li, Z.-J.; Shi, Y.; Yang, Y.-P. Nonlinear characteristics of induced spontaneous combustion process of sulfide ores. *J. Cent. South Univ.* **2016**, *23*, 3284–3292. [[CrossRef](#)]
11. Liu, H.; Wang, Z.; Zhong, J.; Xie, Z. Early detection of spontaneous combustion disaster of sulphide ore stockpiles. *Teh. Vjesn.* **2015**, *22*, 1579–1587.
12. Xiang, C.; Liu, H.; Mu, J.; Lang, Z.; Wang, H.; Nie, R.; Kong, F. Thermodynamic model and kinetic compensation effect of spontaneous combustion of sulfur concentrates. *ACS Omega* **2020**, *5*, 20618–20629. [[CrossRef](#)] [[PubMed](#)]
13. Liu, H.; Xiang, C.; Hong, R.; Song, Y.; Jin, K.; Zhu, K.; Yang, C.; Lv, C. Thermal behavior and kinetics of sulfide concentrates. *Therm. Sci.* **2019**, *23*, 2801–2811. [[CrossRef](#)]
14. Mitishova, N.A. Development of technological recommendations for ensuring fire and explosion safety during underground development of pyrite ore deposits. *Proc. Tula States Univ. Sci. Earth* **2021**, *4*, 165–177.
15. Kaihuan, Z.; Fuchuan, J. Research on intrinsic safety method for open-pit mining. *Procedia Eng.* **2012**, *43*, 453–458. [[CrossRef](#)]
16. Deng, J.; Lue, H.F.; Xiao, Y.; Wang, C.P.; Shu, C.M.; Jiang, Z.G. Thermal effect of ionic liquids on coal spontaneous combustion. *J. Therm. Anal. Calorim.* **2019**, *138*, 3415–3424. [[CrossRef](#)]
17. Xi, X.; Shi, Q.L.; Jiang, S.G.; Zhang, W.Q.; Wang, K.; Wu, Z.Y. Study on the effect of ionic liquids on coal spontaneous combustion characteristic by microstructure and thermodynamic. *Process. Saf. Environ. Protect.* **2020**, *140*, 190–198. [[CrossRef](#)]
18. Wang, L.-Y.; Xu, Y.-L.; Jiang, S.-G.; Yu, M.-G.; Chu, T.-X.; Zhang, W.-Q.; Wu, Z.-Y.; Kou, L.-W. Imidazolium based ionic liquids affecting functional groups and oxidation properties of bituminous coal. *Saf. Sci.* **2012**, *50*, 1528–1534. [[CrossRef](#)]
19. Cui, C.; Jiang, S.; Wang, K.; Zheng, S.; Li, M.; Zhang, W.; Tang, H. Effects of ionic liquid concentration on coal low-temperature oxidation. *Energy Sci. Eng.* **2019**, *7*, 2165–2179. [[CrossRef](#)]
20. Zheng, X.; Zhang, S.; Li, W.; Gong, M.; Yin, L. Experimental and theoretical studies of two imidazolium-based ionic liquids as inhibitors for mild steel in sulfuric acid solution. *Corros. Sci.* **2015**, *95*, 168–179. [[CrossRef](#)]
21. Liu, H.; Hong, R.; Xiang, C.; Wang, H.; Li, Y.; Xu, G.; Chang, P.; Zhu, K. Thermal decomposition kinetics analysis of the oil sludge using model-based method and model-free method. *Process. Saf. Environ. Protect.* **2020**, *141*, 167–177. [[CrossRef](#)]
22. Xi, Z.; Shan, Z.; Li, M.; Wang, X. Analysis of coal spontaneous combustion by thermodynamic methods. *Combust. Sci. Technol.* **2021**, *193*, 2305–2330. [[CrossRef](#)]
23. Hu, R.; Shi, Q. *Thermal Analysis Kinetics*; Science Press: Beijing, China, 2008.
24. Selvaratnam, M.; Garn, P.D. Kinetics of thermal decompositions-improvement in data treatment. *J. Am. Ceram. Soc.* **1976**, *59*, 376. [[CrossRef](#)]
25. Liu, H.; Xiang, C.; Mu, J.; Yao, J.; Ye, D.; Jin, K.; Lang, Z. Thermodynamic model and kinetic compensation effect of oil sludge pyrolysis based on thermogravimetric analysis. *Therm. Sci.* **2022**, *26*, 259–272. [[CrossRef](#)]
26. Luo, L.; Guo, X.; Zhang, Z.; Chai, M.; Rahman, M.; Zhang, X.; Cai, J. Insight into pyrolysis kinetics of lignocellulosic biomass: Isoconversional kinetic analysis by the modified friedman method. *Energy Fuels* **2020**, *34*, 4874–4881. [[CrossRef](#)]
27. Vyazovkin, S.; Burnham, A.K.; Criado, J.M.; Pérez-Maqueda, L.A.; Popescu, C.; Sbirrazzuoli, N. ICTAC Kinetics Committee recommendations for performing kinetic computations on thermal analysis data. *Thermochim. Acta* **2011**, *520*, 1–19. [[CrossRef](#)]
28. Liu, H.; Zhao, S.; Xie, Z.; Zhu, K.; Xu, X.; Ding, X.; Glowacz, A. Investigation of the pyrophoric tendency of the powder of corrosion products in an oil tank. *Powder Technol.* **2018**, *339*, 296–305. [[CrossRef](#)]
29. Liu, H.; Hong, R.; Lang, Z.; Yao, J.; Ye, D.; Shan, J.; Liu, X. Evaluation of the spontaneous combustion tendency of corrosion products in oil tanks based on TOPSIS methodologies. *J. Loss Prev. Process. Ind.* **2021**, *71*, 104475. [[CrossRef](#)]